Self-Assembly of Copper Polypyridyl Supramolecular Metallopolymers to Achieve Enhanced Anticancer Efficacy

Lanhai Lai[+], Dong Luo[+], Ting Liu, Wenjie Zheng, Tianfeng Chen,* and Dan Li*[a]

Self-assembled functional supramolecular metallopolymers have demonstrated application potential in cancer therapy. Herein, a copper polypyridyl complex was found able to self-assemble into a supramolecular metallopolymer driven by the intermolecular interactions, which could enhance the uptake in cancer cells through endocytosis, and thus effectively inhibiting tumor growth in vivo without damaging to the major organs. This study provides a facile way to achieve enhanced anticancer efficacy by using self-assembled metallopolymers.

With purpose to improve material properties, metallopolymers have attracted increasing interest for their potential to supply advanced functional materials for a wide range of applications.[1] Supramolecular polymers, originating from the integration of polymers and supramolecules, are becoming a rapidly developing research area.[2] Supramolecular metallopolymers received increasing attention, partly motivated by their ready-to-form self-assembly[3] and diverse applications in electrochromic materials,[4] luminescent,[5] accelerated guest adsorption,[6] interesting magnetic properties,[7] and other applications.[8] Weak noncovalent interactions, such as hydrogen-bonding, hydrophobic-hydrophobic, metal-metal and π-π interactions,[9] have been identified as driving forces to stabilize the self-assembled structures of metallopolymers.[3a,10] Studies also showed that most metallopolymers were under thermodynamically changing processes with change of temperature.[5a,10a,11] Until now, many supramolecular metallopolymers of gold, copper and platinum complexes, have been well documented,[3c,8a,10b,12] and the search for application potential has become new research focus.

While most of supramolecular metallopolymers are "high-molecular-weight" with relatively large ligands,[13] the discovery of low molecular-weight metallopolymers with tunable structures have fostered a new growth in recent years.[14] Recent studies revealed that a low-molecular-weight metallopolymer in nanofiber form has potent anticancer properties.[8a,15] The nano-formulation has been shown to be able to improve the stability and selectivity of metal complexes, and hence emerges as an appealing strategy to increase anticancer activity and reduce the toxic side effects of these compounds.[16] Therefore, the formation of nanostructures of metallopolymers could have a promising improvement on the biological activities. Recently, studies have found that, metal complexes with 2-phenylimidazo[4,5-f]-[1,10]phenanthroline (pip) as ligand displayed potent anticancer activities.[15,17]

Possibly, the plane structure and NH group of the ligand could form π-π interactions and hydrogen bonds between adjacent molecules. Interestingly, in this study, we synthesized a simple Cu(II) complex, [CuCl(pip)$_2$]Cl, capable of self-assembling into a metallopolymer driven by diverse intermolecular interactions, which demonstrated potent in vivo anticancer efficacy. The Addition of pip in ethanol to CuCl$_2$ in water at ratio of 5:1 and 5:2 resulted in a clear green solution (Figure S1). The solution turned to be viscous after 2 h at room temperature. Upon cooling in a refrigerator, a stable green viscous solution was formed (Figure 1a). When the viscous solution
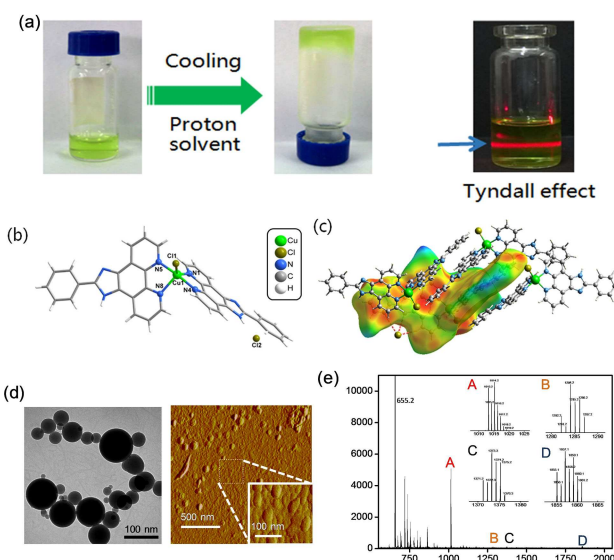
[a] L. Lai,[+] D. Luo,[+] Dr. T. Liu, Prof. W. Zheng, Prof. T. Chen, Prof. D. Li
Department of Chemistry
Jinan University
Guangzhou 510632, GuangDong Province (China)
.
E-mail: tchentf@jnu.edu.cn
         danli@jnu.edu.cn
[+] These authors contributed equally to this work.

Figure 1. [CuCl(pip)$_2$]Cl: (a) Formation of the viscous fluid upon cooling in ethanol/water (v/v = 5:1) and its Tyndall effect. (b) Molecular structure (c) Illustration of Hirshfeld surface in the crystal packing: the mapping range is shown from red (short distance) through green to blue (long distance). (d) TEM images and AFM image of metallopolymer. (e) MALDI-TOF-MS analysis of the [CuCl(pip)$_2$]Cl in ethanol/water (5:1). Insets specific peaks representing different aggregation patterns.

stood at room temperature for 25 days, green single crystals suitable for X-ray diffraction could be obtained in a capped vial. The crystal structure was solved, and its crystallographic data (Table S1) and bond angles/ distances (Table S2) are showed in SI. The crystal unit of [CuCl(pip)$_2$]Cl is in a trigonal pyramidal coordination geometry (Figure 1b).

Hirshfeld surface[18] clearly illustrates that rich supramolecular interactions of conjugated π-π interactions, C(N)—H···Cl hydrogen bonds, and edge-to-face C—H···π interactions are involved (Figure 1c and Figure S2) in the crystal packing. These results indicate that weak interactions including cooperative π-π and multiple unconventional C—H···X hydrogen-bonding interactions are strong enough to from the metallopolymer. UV/Vis and FT-IR spectroscopy was employed to examine the intermolecular aggregation of [CuCl(pip)$_2$]Cl during the assembly process. As shown in Figure S3, UV/Vis spectra of the complex in CH$_3$CH$_2$OH/H$_2$O (5:1) exhibits a red shift with peaks from 409 to 423 nm when the concentration increased. This is ascribed to the enhancement of molecular interactions due to the increase of the concentration. The FT-IR spectra of [CuCl(pip)$_2$]Cl displayed significant difference in different solvents (Figure S4). The red shifts in proton solvent could be attributed to the enhancement of C—H···X hydrogen bond and π–π interaction.

Tyndall effect was observed in the solution of [CuCl(pip)$_2$]Cl in proton solvent CH$_3$CH$_2$OH/H$_2$O (Figure 1a, right), indicating the formation of self-assembled species,[19] while no Tyndall phenomenon observed in aprotic solvent DMF. Therefore, the presence of proton solvent could be a determining factor for the self-assembly, as proton solvent could provide H atom feasible for the aggregation driven by hydrogen bond. In contrast, Tyndall phenomenon could not be observed in the solution of 0.8 mM (Figure S5a), possibly due to the unfavourable intermolecular distances in a dilute solution. Moreover, the mean size of the metallopolymer was found at about 95 nm (Figure S5b), indicating the presence of nanoscale aggregates in this solution. From the TEM images, we found that metallopolymer were highly monodisperse with the size of 83 nm in diameter. And AFM measurement confirmed the spherical nanoparticle morphology of the supramolecular metallopolymer in the proton solvent (Figure 1d). The metallopolymer was further confirmed by XRD (Figure S6). The results of MALDI-TOF-MS analysis also demonstrated the presence of monomeric species, and dimer and trimer aggregation peaks of [CuCl(pip)$_2$]Cl (Figure 1e).

To further understand the phase transition, the effects of temperature, concentration and solvent on the viscosity of [CuCl(pip)$_2$]Cl were examined by Ubbelodhe viscometry. Significant temperature-, solvent- and concentration-dependent changes in the viscosity were recorded (Figure 2 and Figure S7). The stacking mode of [CuCl(pip)$_2$]Cl showing hydrogen bonds (C—H···Cl = 3.681 Å; N—H···Cl = 3.279 Å) and π-π interactions (3.524–3.777 Å) (Figure 2a). High viscosity was detected when incubating in CH$_3$CH$_2$OH/H$_2$O (5:1), which decreased obviously when the temperature increased from 5 °C to 75 °C. However, the viscosity showed no significant increase in aprotic solvent DMF (Figure 2b). Additionally, the decreased viscosity induced
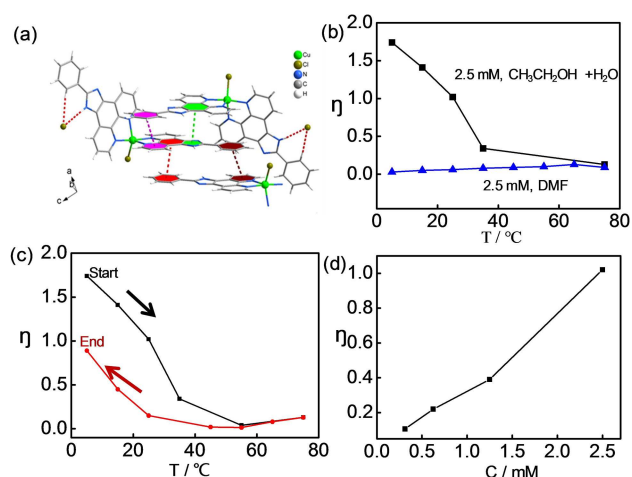

Figure 2. (a) The stacking mode of [CuCl(pip)$_2$]Cl showing hydrogen bonds (C—H…Cl = 3.681 Å; N—H···Cl = 3.279 Å) and π-π interactions (3.524–3.777 Å). Viscosity change of [CuCl(pip)$_2$]Cl. (b) in different solvents and temperatures. (c) dynamic change with temperature varying in the cycle 5–75-5 °C in ethanol/water (5:1) concentration-dependent at 25 °C (d). with different concentration

by rising temperature when the temperature decreased from 75 °C to 5 °C (Figure 2c), which demonstrated the recovering ability of the metallopolymer. The viscosity of [CuCl(pip)$_2$]Cl increased dramatically upon increasing the concentration, which confirms the contribution of enhanced intermolecular interactions during the self-assembly of the metallopolymer (Figure 2d).Further studies were also carried out to examine the effects of the matter forms (metallopolymer and monomeric complex) on the anticancer activity of [CuCl(pip)$_2$]Cl, by in vitro and in vivo models as previously described.[16c,20] As shown in Figure 3a and Figure S8, the metallopolymer demonstrated much higher anticancer activities against the tested cancer cells than the monomeric complex. To understand the reasons accounting for the different activities induced by the matter forms, we compared their cellular uptake in HepG-2 hepatocellular carcinoma cells. Consistently, the metallopolymer exhibited much higher cellular uptake than monomeric complex in different time points (Figure 3b). From the Figure 3c, we found that significant concentration-dependent changes in the cellular uptake were recorded. It is likely that, metallopolymer could assembly into nanoparticles, which enter cancer cells through endocytosis in a high efficiency, thus increasing the cellular uptake and anticancer efficacy. Moreover, the results of Confocal fluorescence images revealed that, the metallopolymer were internalized by cancer cells through endocytosis, and could be released into cytoplasm after 12–24 h (Figure S9).

Furthermore, we assessed the in vivo therapeutic efficacy of the metallopolymer in HepG-2 xenografts nude mice. In this study, metallopolymer was dispersed in PBS and injected into the tumor-bearing nude mice intravenously. As shown in Figures 4 and Figure. S10, the metallopolymer significantly inhibited the tumor growth, as evidenced by the decrease in tumor volume and tumor weight in a time-dependent manner. Moreover, under the effective dose, the metallopolymer
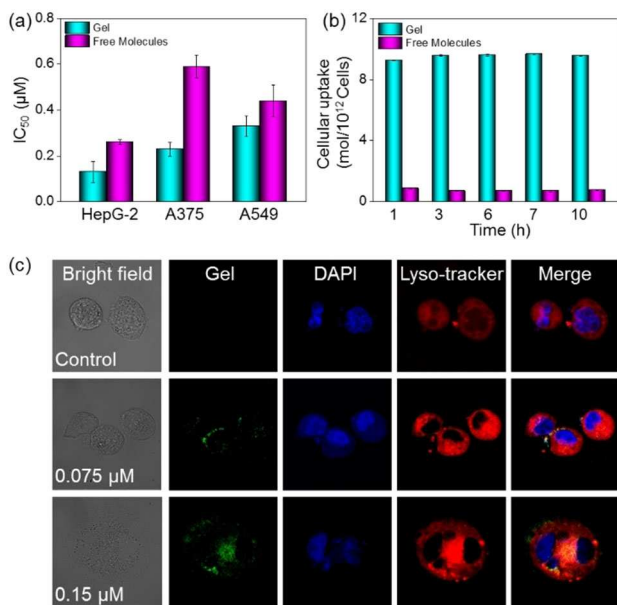
Figure 3. (a) Cytotoxic effects of monomeric [CuCl(pip)$_2$]Cl and metallopolymer on different cancer cells (72 h). (b) Time-course cellular uptake of monomeric [CuCl(pip)$_2$]Cl, metallopolymer in HepG-2 cells (10 μM). (c) Cellular uptake of metallopolymer by Confocal fluorescence images.

showed no damage to these major organs, including heart, liver, spleen, lung and kidney (Figure 4d), demonstrating the
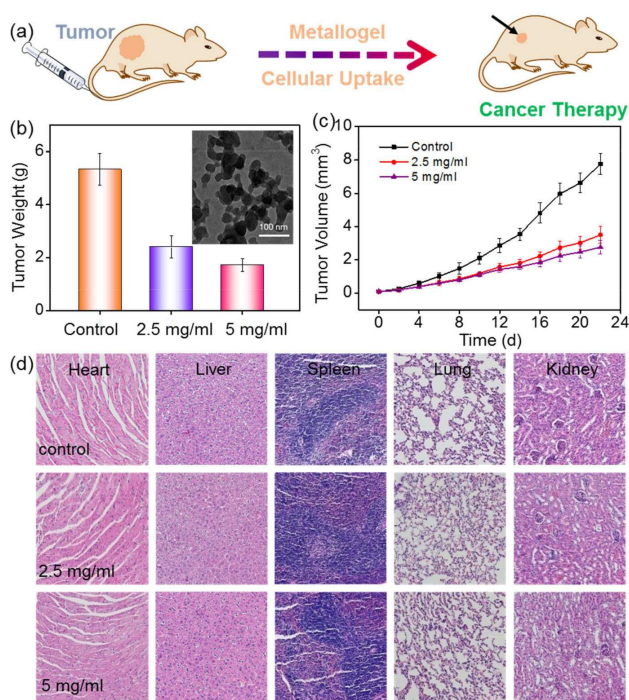

Figure 4. (a) Schematic demonstration for tumor growth inhibition by metallopolymer. (b, c) *In vivo* anticancer activity of the metallopolymer against HepG-2 cells xenografts. Inset is TEM images of the metallopolymer in DMEM medium (24 h). (d) H&E staining of major organs after treatments.

cancer therapeutic potential and safety of this kind of self-assembled functional metallopolymer.

In summary, a simple Cu(II) complex, [CuCl(pip)$_2$]Cl, was found be able to self-assemble into surpramolecular metallopolymers driven by diverse intermolecular interactions, including π–π interactions and hydrogen bonds under a proton solvent condition. The functional metallopolymer could enter cancer cells through endocytosis, thus effectively inhibit tumor growth in vivo without damage to the major organs. Taken together, this study provides a facile way to achieve enhanced anticancer efficacy by using self-assembled metallopolymer.

Acknowledgements

Conflict of Interest

The authors declare no conflict of interest.

[1] a) A. Winter, U. S. Schubert, *Chem. Soc. Rev.* **2016**, *45*, 5311–5357; b) S. Theis, A. Iturmendi, C. Gorsche, M. Orthofer, M. Lunzer, S. Baudis, A. Ovsianikov, R. Liska, U. Monkowius, I. Teasdale, *Angew. Chem. Int. Ed. Engl.* **2017**, *56*, 15857–15860.

[2] a) L. Yang, X. Tan, Z. Wang, X. Zhang, *Chem. Rev.* **2015**, *115*, 7196–7239; b) A. Y. Tam, V. W. Yam, *Chem. Soc. Rev.* **2013**, *42*, 1540–1567; c) P. Wei, X. Yan, F. Huang, *Chem. Soc. Rev.* **2015**, *44*, 815–832; d) Q. Lin, T. T. Lu, X. Zhu, B. Sun, Q. P. Yang, T. B. Wei, Y. M. Zhang, *Chem. Commun.* **2015**, *51*, 1635–1638; e) F. Huang, O. A. Scherman, *Chem. Soc. Rev.* **2012**, *41*, 5879–5880.

[3] a) C. Rest, M. J. Mayoral, K. Fucke, J. Schellheimer, V. Stepanenko, G. Fernandez, *Angew. Chem. Int. Ed. Engl.* **2014**, *53*, 700–705; b) T. D. Hamilton, D. K. Bucar, J. Baltrusaitis, D. R. Flanagan, Y. Li, S. Ghorai, A. V. Tivanski, L. R. MacGillivray, *J. Am. Chem. Soc.* **2011**, *133*, 3365–3371; c) W. Fang, Z. Sun, T. Tu, *J. Phys. Chem. C* **2013**, *117*, 25185–25194.

[4] C. W. Hu, T. Sato, J. Zhang, S. Moriyama, M. Higuchi, *J. Mater. Chem. C* **2013**, *1*, 3408–3413.

[5] a) X. de Hatten, N. Bell, N. Yufa, G. Christmann, J. R. Nitschke, *J. Am. Chem. Soc.* **2011**, *133*, 3158–3164; b) D. Asil, J. A. Foster, A. Patra, X. de Hatten, J. del Barrio, O. A. Scherman, J. R. Nitschke, R. H. Friend, *Angew. Chem. Int. Ed. Engl.* **2014**, *53*, 8388–8391; c) Y. J. Yadav, B. Heinrich, G. De Luca, A. M. Talarico, T. F. Mastropietro, M. Ghedini, B. Donnio, E. I. Szerb, *Adv. Opt. Mater.* **2013**, *1*, 844–854.

[6] D. Tanaka, A. Henke, K. Albrecht, M. Moeller, K. Nakagawa, S. Kitagawa, J. Groll, *Nat. Chem.* **2010**, *2*, 410–416.

[7] M. Kurmoo, *Chem. Soc. Rev.* **2009**, *38*, 1353–1379.

[8] a) J.-J. Zhang, W. Lu, R. W.-Y. Sun, C.-M. Che, *Angew. Chem. Int. Ed. Engl.* **2012**, *124*, 4966–4970; b) X. de Hatten, D. Asil, R. H. Friend, J. R. Nitschke, *J. Am. Chem. Soc.* **2012**, *134*, 19170–19178.

[9] a) M. L. Bushey, T. Q. Nguyen, W. Zhang, D. Horoszewski, C. Nuckolls, *Angew. Chem. Int. Ed. Engl.* **2004**, *43*, 5446–5453; b) C. Po, Z. H. Ke, A. Y. Y. Tam, H. F. Chow, V. W. W. Yam, *Chem. Eur. J.* **2013**, *19*, 15735–15744; c) X. Yan, T. R. Cook, J. B. Pollock, P. Wei, Y. Zhang, Y. Yu, F. Huang, P. J. Stang, *J. Am. Chem. Soc.* **2014**, *136*, 4460–4463; d) A. Y. Tam,

K. M. Wong, N. Zhu, G. Wang, V. W. Yam, *Langmuir* **2009**, *25*, 8685–8695; e) M. J. Mayoral, C. Rest, V. Stepanenko, J. Schellheimer, R. Q. Albuquerque, G. Fernández, *J. Am. Chem. Soc.* **2013**, *135*, 2148–2151; f) A. Y.-Y. Tam, K. M.-C. Wong, G. Wang, V. W.-W. Yam, *Chem. Commun.* **2007**, 2028; g) C. M. Leenders, T. Mes, M. B. Baker, M. M. Koenigs, P. Besenius, A. R. Palmans, E. Meijer, *Mater. Horiz.* **2014**, *1*, 116–120.

[10] a) A. Y.-Y. Tam, K. M.-C. Wong, V. W.-W. Yam, *J. Am. Chem. Soc.* **2009**, *131*, 6253–6260; b) H. L. Au-Yeung, S. Y. Leung, A. Y. Tam, V. W. Yam, *J. Am. Chem. Soc.* **2014**, *136*, 17910–17913.

[11] E. R. Janecek, J. R. Mckee, C. S. Y. Tan, A. Nykanen, M. Kettunen, J. Laine, O. Ikkala, O. A. Scherman, *Angew. Chem. Int. Ed.* **2015**, *54*, 5383–5388; *Angew. Chem.* **2015**, *127*, 5473–5478.

[12] a) T. Cardinaels, J. Ramaekers, P. Nockemann, K. Driesen, K. Van Hecke, L. Van Meervelt, S. Lei, S. De Feyter, D. Guillon, B. Donnio, K. Binnemans, *Chem. Mater.* **2008**, *20*, 1278–1291; b) Y. M. Yamada, S. M. Sarkar, Y. Uozumi, *J. Am. Chem. Soc.* **2012**, *134*, 3190–3198; c) Z. X. Liu, Y. Feng, Z. Y. Zhao, Z. C. Yan, Y. M. He, X. J. Luo, C. Y. Liu, Q. H. Fan, *Chem. Eur. J.* **2014**, *20*, 533–541; d) A. C. Jackson, S. D. Walck, K. E. Strawhecker, B. G. Butler, R. H. Lambeth, F. L. Beyer, *Macromolecules* **2014**, *47*, 4144–4150; e) W. J. Gee, S. R. Batten, *Chem. Commun.* **2012**, *48*, 4830–4832.

[13] Y. K. Tian, Y. G. Shi, Z. S. Yang, F. Wang, *Angew. Chem. Int. Ed.* **2014**, *53*, 6090–6094; *Angew. Chem.* **2014**, *126*, 6204–6208.

[14] a) W. Wang, Q. Chen, Q. Li, Y. Sheng, X. Zhang, K. Uvdal, *Cryst. Growth Des.* **2012**, *12*, 2707–2713; b) R. Y. Kuwahara, H. Yamagishi, K. Hashimoto, S. Tamesue, T. Yamauchi, N. Tsubokawa, *Polymer* **2015**, *61*, 99–107; c) S. Bhowmik, B. N. Ghosh, V. Marjomaki, K. Rissanen, *J. Am. Chem. Soc.* **2014**, *136*, 5543–5546; d) M. Dudek, J. K. Clegg, C. R. K. Glasson, N. Kelly, K. Gloe, K. Gloe, A. Kelling, H.-J. R. Buschmann, K. A. Jolliffe, L. F. Lindoy,

G. V. Meehan, *Cryst. Growth Des.* **2011**, *11*, 1697–1704; e) S. Bhattacharya, S. Sengupta, S. Bala, A. Goswami, S. Ganguly, R. Mondal, *Cryst. Growth Des.* **2014**, *14*, 2366–2374; f) D. Yan, D. G. Evans, *Mater. Horiz.* **2014**, *1*, 46–57.

[15] J. L.-L. Tsai, T. Zou, J. Liu, T. Chen, A. O.-Y. Chan, C. Yang, C.-N. Loka, C.-M. Che, *Chem. Sci.* **2015**, *6*, 3823–3830.

[16] a) W. Liu, X. Li, Y.-S. Wong, W. Zheng, Y. Zhang, W. Cao, T. Chen, *ACS Nano* **2012**, *8*, 6578–6591; b) L. Z. He, Y. Y. Huang, H. L. Zhu, G. H. Pang, W. J. Zheng, Y. S. Wong, T. F. Chen, *Adv. Funct. Mater.* **2014**, *24*, 2754–2763; c) Y. Y. Huang, Y. Luo, W. J. Zheng, T. F. Chen, *ACS Appl. Mater. Interfaces* **2014**, *6*, 19217–19228.

[17] a) Z. Zhao, Z. Luo, Q. Wu, W. Zheng, Y. Feng, T. Chen, *Dalton Trans.* **2014**, *43*, 17017–17028; b) T. Chen, Y. Liu, W. J. Zheng, J. Liu, Y. S. Wong, *Inorg. Chem.* **2010**, *49*, 6366–6368; c) L. Xie, Z. Luo, Z. Zhao, T. Chen, *J. Med. Chem.* **2016**, *60*, 202–214; d) Z. Zhao, P. Gao, Y. You, T. Chen, *Chem. Eur. J.* **2017**, *24*, 3289–3298.

[18] M. A. Spackman, *Phys. Scr.* **2013**, *87*, 048103.

[19] L. J. Chen, G. Z. Zhao, B. Jiang, B. Sun, M. Wang, L. Xu, J. He, Z. Abliz, H. Tan, X. Li, H. B. Yang, *J. Am. Chem. Soc.* **2014**, *136*, 5993–6001.

[20] a) Z. Zhao, X. Zhang, C. E. Li, T. Chen, *Biomaterials* **2018**, *192*, 579–589; b) S. Gao, T. F. Chen, M. Y. Choi, Y. W. Liang, J. Y. Xue, Y. S. Wong, *Cancer Lett.* **2013**, *333*, 36–46.